Constraining cosmic curvature by using age of galaxies and gravitational lenses

Akshay Rana[a1], Deepak Jain[b], Shobhit Mahajan[a] and Amitabha Mukherjee[a]
[a]Department of Physics & Astrophysics, University of Delhi, Delhi 110007, India
[b]Deen Dayal Upadhyaya College, University of Delhi, Sector 3, Dwarka, New Delhi 110078, India
[1]Email- arana@physics.du.ac.in

arXiv:1611.07196v1 [astro-ph.CO] 22 Nov 2016

Abstract: We use two model-independent methods to constrain the curvature of the universe. In the first method, we measure the curvature parameter (Ω_k^0) by using the observations of the Hubble parameter and comoving distances obtained from the age of galaxies. Secondly, we also use an indirect method based on the mean image separation statistics of gravitationally lensed quasars. The basis of this methodology is that the average image separation of lensed images will show a positive, negative or no correlation with the source redshift in a closed, open or flat Universe respectively. In order to smoothen the datasets used in both the methods, we use a non-parametric method namely, Gaussian process (GP). However, the bound on the present value of Ω_k^0 obtained from Method I (from age of galaxies) using GP technique is $\Omega_k^0 = -0.22 \pm 0.58$. But the combined result from both the methods suggest that our universe is homogeneous and spatially flat within 3σ level.

Keywords: Curvature density, Age of galaxy, Gravitational Lensing, Image separation, Gaussian process.

1 Introduction

Cosmic curvature is a fundamental parameter in cosmology. It plays a crucial role in the evolution of Universe. Theoretically, inflationary models predict that the radius of curvature of the Universe should be very large, which in turn implies a vanishingly small cosmic curvature. Furthermore, the combined observational constraints by SNe Ia, BAO, Hubble Data and WMAP survey also suggest that Ω_k is indeed very small [1]. Recently, Planck survey has given very precise bounds on curvature density, $\Omega_k = 0.000 \pm 0.005$ (95%, Planck TT+lowP+lensing+BAO) [2]. Though the flatness of Universe obtained from the cosmological observations is almost at an unprecedented level of precision, it's interpretation still depends on the fact that the background cosmology is explained by homogeneous and isotropic FLRW metric. In order to test the FLRW metric and curvature of the universe, Clarkson et al proposed that any detection of redshift dependence of curvature parameter would imply presence of non FLRW cosmology [3].

Another important issue is the presence of the geometric degeneracy between dark energy equation of state parameter $w(z)$ and cosmic curvature Ω_k. This degeneracy prevent us to understand the nature of dark energy. To circumvent this problem, most of the work neglects Ω_k (by advocating that several observations put very small bounds on Ω_k) and attempts to find bounds on $w(z)$ independently. However, it has been found that ignoring Ω_k leads to errors in the reconstruction of $w(z)$ and even a small value of Ω_k induces a large effect at higher redshifts $z \simeq 1$. Hence it seems inconsistent to neglect the contribution of Ω_k, howsoever small it might be. [4]. Moreover many dark energy tests such as the Integrated Sachs-Wolfe (ISW) effect and cluster surveys are also very sensitive to the assumption about Ω_k [5]. In addition, many alternate theories (theories based on the anthropic principle [6], the Inhomogeneous Universe [7] and the Irrotational dust universe [8] etc.) have been proposed to address the fine tuning of parameters and the presence of dark energy. Furthermore, a precise measure of cosmic curvature ($|\Omega_k^0| < 10^{-4}$) can act as a excellent test for several inflationary models of the universe [9–11]. Hence it is very important to constrain the Ω_k in a model independent manner.

In this paper, we use two different model independent techniques to estimate the curvature of the universe. Firstly in Method I, we determine the Ω_k by using the independent dataset of Hubble parameter $H(z)$ and the comoving distance obtained by using the age of galaxies [12]. A prominent feature of this analysis is that it doesn't rely on any assumption of the underlying cosmological model. If we find any deviation in the evolution of cosmic curvature then it is an indication of new physics . We apply Gaussian Process (GP) smoothing technique to the data points to infer any violation of FLRW based cosmological models. In Method II, Ω_k is constrained by using the statistical properties of gravitational lens systems. Gott, Park and Lee showed that for the Singular Isothermal Spherical (SIS) model of galaxies, the mean image separation $< \Delta\theta >$ is independent of the source redshift if the Universe is assumed to be flat in FLRW Universe [13]. We use a updated dataset of 44 gravitational lenses from the DR7 SDSS gravitational lens dataset [14]. We again apply the non-parametric technique of Gaussian Process on the image separation data points to constrain the cosmic curvature.

The structure of the paper is as follows: In Section 2 , we discuss the Method I based on the determination of the cosmic curvature in a model independent manner and methodology to obtain the comoving distance from the age of galaxies. In Section 3, we explain the Method II which is based on the image separation statistics of gravitationally lensed quasars. We analyze the results in Section 4.

2 Method I : Null test of cosmic curvature using $H(z)$ and age of galaxies

This method provide a model independent test of spatial curvature of the universe. It is based on a geometrical relation between the Hubble parameter $H(z)$, comoving distance $r(z)$ and its first derivative $r'(z)$. It enable us to check whether the present curvature density is independent of the redshift of measurement or not. This test was firstly proposed by Clarkson.et.al [3] and further used by several authors [15–22] where independent observations of Hubble parameter and comoving distances are used to constrain the cosmic curvature. The relation is given as ;

$$\Omega_k^0 = \frac{H(z)^2 r'(z)^2 - c^2}{H_0^2 r(z)^2} \tag{1}$$

It measure the present curvature density by using the independent observations of $H(z)$ and comoving distance at one single redshift. In any FLRW Universe, the curvature parameter remains independent of redshift of measurement. In other words, If the present curvature parameter is found to be dependent on the redshift of measurement, then there is a need to explore the models beyond FLRW metric. The above Eq.1 provide us the simplest way to analyze the present cosmic curvature by using the independent measurements of $H(z)$, $r(z)$ and $r'(z)$ at a given redshift. In the next subsection we will see how to generate these datasets.

2.1 Estimating the comoving distance using the age-redshift dataset of galaxies

The comoving distance $r(z)$ can be obtained from the age-redshift data of galaxies [12]. FLRW cosmology enables us to write down the comoving distance $r(z)$ in the form of first derivative of the age of galaxy,

$$r(z) = c \int_z^0 \left[(1+z) \frac{dt}{dz} \right] dz \tag{2}$$

where t is the age of universe at redshift z. If one can determine $\frac{dt}{dz}$ at the required redshift then one can easily reconstruct the value of comoving distance $r(z)$. For this purpose we use an age-redshift

dataset of 32 old, passive galaxies distributed over the redshift interval of $0.11 < z < 1.84$. Further we add an incubation time $t_{inc} = 1.5 \pm 0.45$ Gyr that accounts for the time from the beginning of the universe to the formation of the first galaxy. This is the mean value of the incubation bound obtained by Wei et. al. [23] using the age of a galaxy sample in a flat Λ CDM model. However, a 12% error is given in the analysis of measurement of age of galaxies which we take as the uncertainty in measurement [24–26].

The present age of universe is taken to be 13.79 ± 0.021 Gyr obtained by Planck survey with a joint analysis of CMB + BAO + SNe Ia + H_0 [2]. Once we have the dataset, we fit this data using a third degree polynomial $t(z) = A + Bz + Cz^2 + Dz^3$. The best fit values turn out to be (in Gyr): $A = 13.78 \pm 0.01$, $B = -13.50 \pm 0.84$, $C = 7.37 \pm 1.19$, $D = -1.63 \pm 0.48$ with a $\chi^2_\nu = 0.3$. The best fit curve is shown in Fig. 1.

On differentiating the polynomial, we obtain $\frac{dt}{dz} = B + 2Cz + 3Dz^2$. Hence by using Eq. 2, we get the comoving distance :

$$r(z) = c\left[-B\left(z + \frac{z^2}{2}\right) - C\left(z^2 + \frac{2z^3}{3}\right) - D\left(z^3 + \frac{3z^4}{4}\right)\right] \tag{3}$$

and on further differentiating it, we get

$$r'(z) = c\left[-B\left(1 + z\right) - 2C\left(z + z^2\right) - 3D\left(z^2 + z^3\right)\right] \tag{4}$$

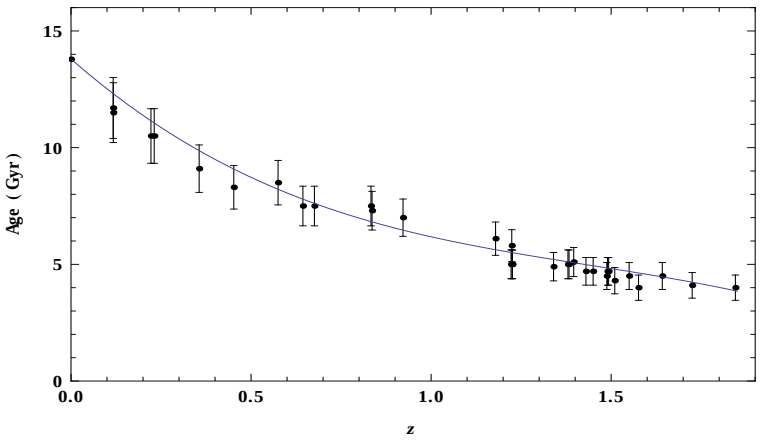

Figure 1: Age of galaxy $t(z)$ vs z . The black points are the original data of 32 points added with an incubation time $t_{inc} = 1.50 \pm 0.45$ Gyr. The blue line is obtained from the fit by using a third degree polynomial.

2.2 Dataset and methodology

In order to derive the value of Ω_k^0 by using the observations at different redshift, we need the Hubble data along with comoving distance $r(z)$ and its first derivative $r'(z)$.

2.2.1 Age of galaxy dataset

To find the comoving distance $r(z)$ and its derivative $r'(z)$, we use 32 data points of age of galaxy ($0.11 < z < 1.84$) plus one data point from the Planck survey for the present age of the Universe . Out of these 32 data-points, 20 are red galaxies from the Gemini Deep Survey (GDDS) [27], 10 are early field type galaxies [28] whose age are obtained by using SPEED models [29] and there are two radio galaxies LBDS 53W069 and LBDS 53W091 [30].

2.2.2 Hubble dataset

We use a recent 36 $H(z)$ data points, out of which 7 are derived from the BAO measurements and 29 points are obtained by using the differential age of galaxies [see table 2]. However it is important to stress that in order to derive the value of Ω_k^0 , both the dataset ($H(z)$ and age of galaxies for comoving distances) must be independent of each other. Therefore we have to look for the available Hubble data-points carefully and avoid those points in Hubble data which are already used to derive the comoving distances. It is observe that in Hubble data set , 9 Hubble data-points are obtained by using the same 32 age of galaxy data points or their subsamples, which are used to derive the comoving distances. So we remove these nine points (For details see Table.2) from Hubble dataset. Finally we are left with 27 Hubble data points in the redshift range $0.07 < z < 1.363$.

Now by using these two independent datasets of the Hubble parameter and the comoving distance derived by using the age of galaxies, we reconstruct a dataset of cosmic curvature Ω_k^0 having 27 data points and the corresponding error bars are derived by using the standard error propagation method

$$\sigma^2_{\Omega_k^0} = 4(\Omega_k^0)^2 \left[\left(\frac{\sigma_r}{r}\right)^2 + \left(\frac{\sigma_{H_0}}{H_0}\right)^2 \right] + 4 \left[(\Omega_k^0)^2 + \frac{c^2}{(H_0 r)^2} \right] \left[\left(\frac{\sigma_H}{H}\right)^2 + \left(\frac{\sigma_{r'}}{r'}\right)^2 \right] \tag{5}$$

where σ_r, $\sigma_{r'}$, σ_H and σ_{H_0} are the errors in the comoving distance $r(z)$, its first derivative $r'(z)$, the Hubble parameter H and the present value of Hubble constant H_0 respectively. Here we use the most recent value of $H_0 = 73 \pm 1.75$ km/sec/Mpc given by Riess et. al [31]. We see that at lower redshifts the error in Ω_k^0 are dominated by r^{-4}, due to which large errors occur in the determination of curvature at low redshifts. Similar behaviour of Ω_k^0 at low redshifts has been observed in different datasets of Ω_k^0, derived using the Hubble parameter, SNe Ia [15] and BAO [17]. In order to constrain Ω_k^0, we further remove two observations at very low redshift which are at $z < 0.1$. We are finally left with 25 Ω_k^0 datapoints in the redshift range $0.12 < z < 1.363$ (See Fig.2).

In order to understand the global behavior of Ω_k^0, we employ a non-parametric method, namely Gaussian Process [32, 33] on the newly constructed dataset and obtain a smoothened curve with the corresponding 1σ and 2σ confidence bands. In FLRW cosmology, the present value of Ω_k^0 must be independent of redshift of measurement. So any deviation may hint the opening of new window which can explain background cosmology based on non FLRW metric.

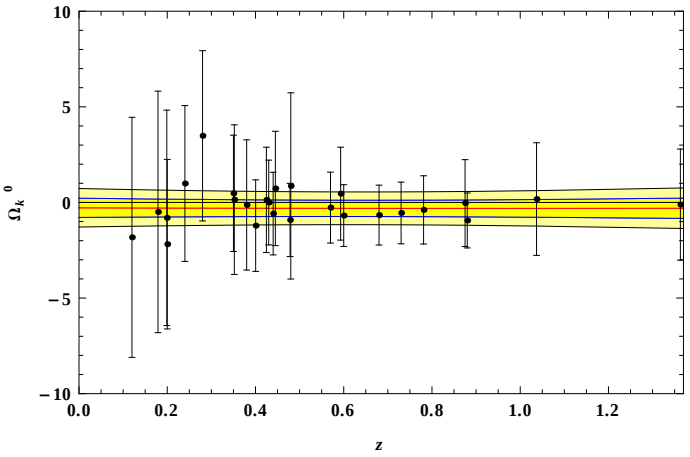

Figure 2: Smooth plot of Ω_k^0 vs z after applying Gaussian Process. Red line shows the best fit line while dark yellow and light yellow regions are the 1σ and 2σ confidence bands respectively. Black points are the 25 reconstructed datapoints of Ω_k^0 at different redshifts.

By analyzing Fig. 2, we observe that Ω_k^0 remains constant in the entire redshift range $0 < z < 1.37$. However the best fit line shows a very small inclination towards the negative value of Ω_k^0 and the present

value of the Ω_k^0 turns out to be equal to -0.22 ± 0.58. The whole reconstructed region also include the flat Universe within the 1σ confidence level. It suggest that the universe can be described with FLRW metric supporting homogeneous universe with flat curvature within 1σ level .

3 Method II : Constraining cosmic curvature using the mean image separation of gravitational lenses

Gravitational lensing is an important observational tool in cosmology. This has the advantage over the other cosmological tools as it relies on relatively well understood physics. Various aspects of the gravitational lensing have been studied elaborately which helps us to understand the geometry and the constituents of the Universe. In their seminal work, TOG (1984) [34] studied the statistical properties of gravitational lenses in order to understand the cosmological parameters and their evolution. One of the important aspects of the statistical properties is the relation between the average image separation and source redshift. In this work, we have exploited this relation to put constraints on the cosmic curvature. This analysis is based on a fact that *the mean image separation is completely independent of the source redshift for the all FLRW based cosmological models in a flat Universe i.e.* $\Omega_k = 0$ *, if the lensing galaxy is non-evolving and modelled as a Singular Isothermal Sphere (SIS). [13, 35–39]* In this case, the normalized mean image separation $\frac{<\Delta\theta(z_s)>}{\Delta\theta_0}$ for the SIS galaxy lenses can be defined as [35–37]

$$\frac{<\Delta\theta(z_s)>}{\Delta\theta_0} = \frac{(\int_0^{z_s} \frac{D_{LS}^3 D_{OL}^2 (1+z_L)^2}{D_{OS}^3 E(z_L)} dz_L)}{(\int_0^{z_s} \frac{D_{LS}^2 D_{OL}^2 (1+z_L)^2}{D_{OS}^2 E(z_L)} dz_L)} \tag{6}$$

where z_L & z_S are the lens and source redshifts respectively. L, S and O represent the lens, source and observer, while D_{LS}, D_{OL} & D_{OS} indicate the corresponding angular diameter distances between the lens , source and observer (for mathematical expressions see [40]). Further $E(z) = H(z)/H_0$ and $\Delta\theta_0 = \frac{8\pi\sigma_v^2}{c^2}$, where $H(z)$ is the Hubble parameter and σ_v is the velocity dispersion of the lens galaxy. [41].

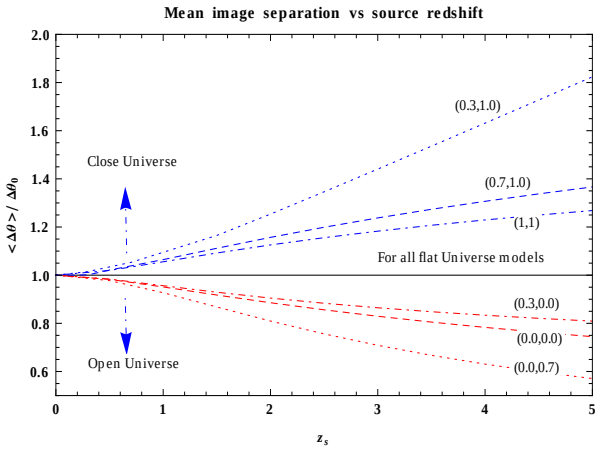

Figure 3: Normalized mean image separation $\frac{<\Delta\theta>}{\Delta\theta_0}$ vs source redshift z_s for different cosmological models. Values in brackets represents the matter density and the cosmological constant density i.e. $(\Omega_m, \Omega_\Lambda)$ configurations, while the black solid line is for all possible flat Universe configurations i.e. $\Omega_m + \Omega_\Lambda = 1$.

In Fig.3, we plot the normalized mean image separation $\frac{<\Delta\theta(z_s)>}{\Delta\theta_0}$ vs source redshift z_s. It shows that for the SIS model of lenses the image separation integrated over the the lens redshift $z_L = 0$ to $z_L = z_S$ is

completely independent of the source redshift z_s for a flat universe. However, the mean image separation decreases with source redshift in an open universe and increases in a closed universe. In a closed universe the volume decreases faster with redshift than in a flat universe, and the source is more likely to be lensed by the lensing galaxies at shorter distances, which in turn produces large image separations, and vice versa for an open universe. The aim of this work is to analyze the present available data for exploring the possible correlation between the average image separation and source redshift. Any correlation will shed some light on the cosmic curvature.

3.1 Dataset and methodology

We use the final statistical sample of lensed quasars from the Sloan Digital Sky Survey (SDSS) Quasar Lens Search (SQLS). This SDSS DR7 quasar catalog consists of 26 a well-defined statistical lens sample and 36 additional lenses identified with various techniques [14]. However as we are assuming the SIS model of galaxies for lenses, this limits the number of source images to two or a perfect Einstein ring. So we select only those lens systems which have two images. Since the image separations in some lens systems are too large which can not be explained comfortably by assuming the SIS lens model [36, 42]. Therefore we impose a selection criterion according to which the maximum image separation between two images should be less than $4''$ [43]. After applying these criteria on a dataset containing 62 lensing systems, we are finally left with 44 galaxy lenses only. For calculating the mean image separation first we divided this dataset in the redshift bin-size of 0.3 and 0.5 each and then determine the mean value of $\Delta\theta$ in each interval (See Fig.5 upper panel). The size of redshift bins are selected in such a way that two or more than two points should lie in each interval. Though a large bin size will increase the bias in the result, we believe that with the availability of more data points in near future may reduces the bias in the result.

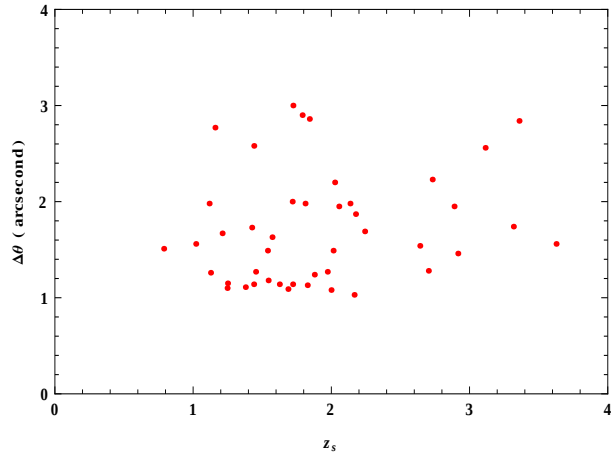

Figure 4: Observed data of statistical sample of lensed quasars from the Sloan Digital Sky Survey (SDSS) Quasar Lens Search (SQLS) (44 data points) after applying selection criteria.

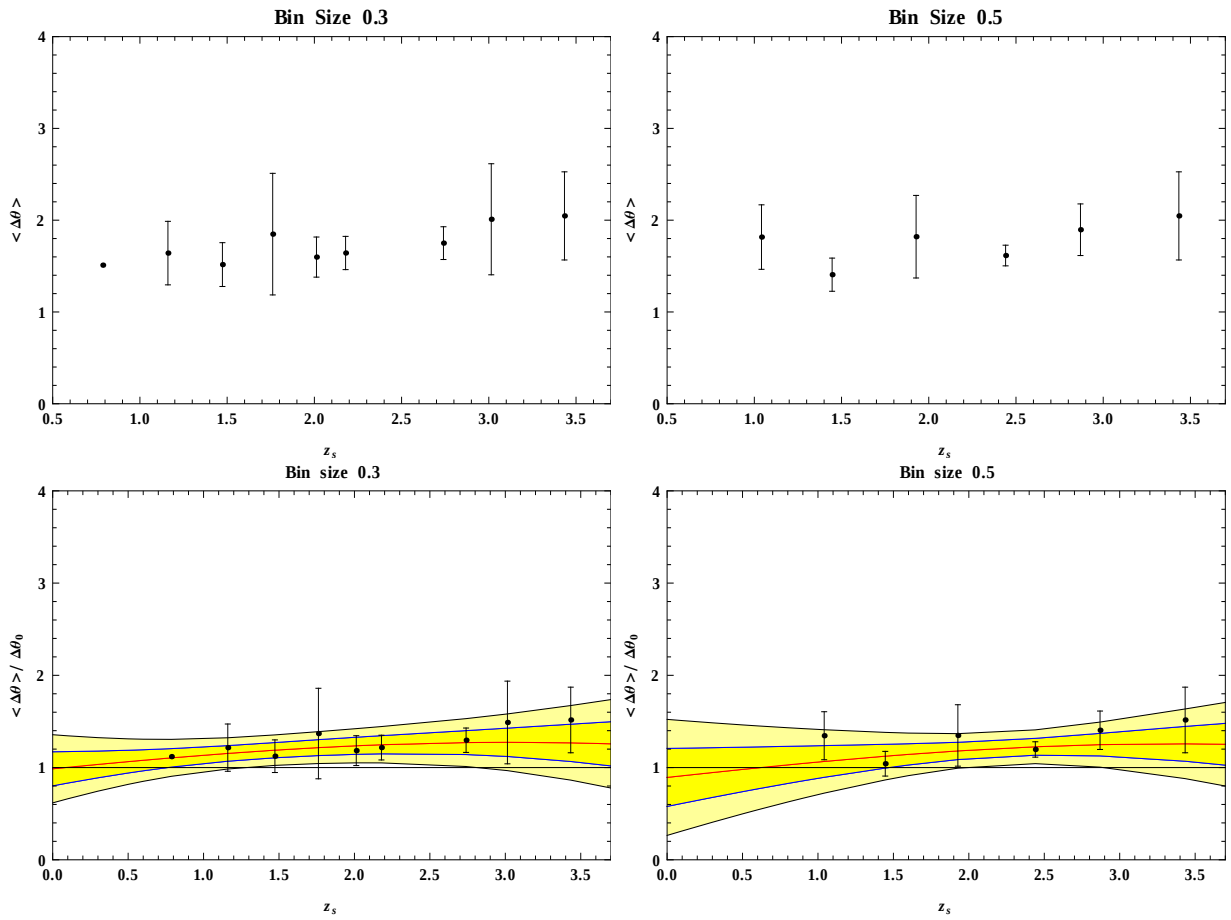

Figure 5: Upper two figures show the formation of different datasets using a binning size of 0.3 (upper left) and 0.5 (upper right) respectively. The lower panel of figures contains the smoothened curve of the normalized mean image separation datasets formed using a binning size 0.3 (left) and 0.5 (right) respectively. Red line shows the best fit line obtained using the Gaussian process with the 1σ and 2σ confidence regions.

In this method, our aim is to make use of the fact that the mean image separation of lensed sources remains constant with respect to the source redshift for all possible flat universe models, if the lensing galaxy follow SIS model. This enables us to differentiate between open, close and flat Universe. In our analysis, we use the image separation of 44 gravitational lenses and further created two datasets of 9 and 6 data points by assuming the redshift bin of size 0.3 and 0.5 respectively. We apply the Gaussian process on these two datasets to study the variation of mean image separation with respect to source redshift. In the flat Universe the reconstructed curves should remain independent of source redshift as shown in Fig.3 and the normalized value of the mean image separation must have a constant value equal to one. However, by analyzing Fig.5, we find that the reconstructed curves are a showing very weak inclination towards a closed Universe. However within the 2σ confidence region, both curves partially include the $\frac{\Delta\theta(z_s)}{\Delta\theta_0} = 1$ line. Thus, we can argue that the best fit line seems to indicate a closed Universe but within the 3σ confidence region it will accommodate the possibility of a flat Universe easily.

To further analyze this correlation between the image separation and the source redshift, we apply three statistical tests to check the correlation between parameters. Pearson product-moment correlation test, Spearman rank correlation test and Kendall rank correlation test are the well established tests which are widely used to check the linearity and monotonicity or in other words, the correlation between two parameters [44]. Out of these three tests, the Pearson product-moment correlation test gives a parametric measure of the degree of linear dependence between two variables and is denoted by the symbol r, while the other two methods of Spearman's rank correlation test and Kendall rank correlation test are a nonparametric measure of the strength and direction of association that exists between two

Statistical tests	value
Spearman's rank coefficient (ρ)	0.22± 0.09
Pearson product-moment coefficient (r)	0.20± 0.15
Kendall rank correlation coefficient (τ)	0.13 ± 0.01

Table 1: Statistical tests to check the correlation between image separation and source redshift.

variables or check their statistical dependence and are represented by ρ and τ respectively. The value of the coefficient corresponding to each test takes a range of values from $+1$ to -1. A value of zero indicates that there is no correlation between the two variables. A value greater and smaller than zero indicates a positive and negative correlation respectively. The value of r, ρ and τ with the corresponding error bars are mentioned in the Table1. Each statistical test indicates a weak positive correlation between image separation $\Delta\theta$ and source redshift z_s. These tests also shows their consistency with the variation of reconstructed curve shown in Fig.5.

4 Results and Discussions

Given the crucial role played by Cosmic curvature in the evolution of the universe, it is important to study the cosmic curvature in a model independent manner. Several methods have been proposed to determine the curvature parameter using different techniques. In this paper, we work on two different approaches. Method I is a Null test of cosmic curvature implemented by using a dataset of the Hubble parameter $H(z)$ and age of galaxies. In this approach, our main focus is to check the assumption of FLRW Universe and homogeneity of Universe. On the other hand, Method II is based on the statistical properties of gravitational lenses. It gives us an indirect window to check the flatness of Universe if FLRW holds. Hence the outcome of Method I paves the way for Method II. In totality, it gives a measure of the consistency of flat Universe based on FLRW metric. Here we will discuss the outcome of both the methods separately.

4.1 Method I

This method is based on a model independent null test of cosmic curvature [3]. This test is presented as a test of homogeneity of Universe. It highlights the importance of measuring the cosmic curvature in a more precise manner. In addition, weak lensing and baryon accoustic oscillation (BAO) datasets have also been used to constrain the cosmic curvature based on the distance sum rule [45, 46]. However, the efficiency of this test is limited because of the large uncertainties in the weak gravitational lensing datasets.

The main logic behind the null test of curvature is the fact that if we have two mutually independent datasets of the Hubble parameter $H(z)$ and the comoving distance simultaneously, then we can reconstruct the present value of the cosmic curvature at each redshift of measurement. In a FLRW Universe Ω_k^0 should not depend on the redshift and if we observe any deviation from this, then it is a direct indication of deviation from a FLRW Universe or a violation of the assumption of homogeneity of the Universe [15, 47]. Efforts have been made to relate a violation of this null test of cosmic curvature to the inhomogeneous cosmology model [48]. Further Bohem et.al (2013) have presented the violation of this null nest of curvature as a signature of back-reaction toy model with realistic features and have tried to confront it with the Union2.1 supernova data [49].

The main challenge is to check the efficiency of this null test in a precise manner. Earlier Union2.0 SNe Ia dataset was used for calculating the comoving distance and the Hubble parameter data points are obtained from differential ages of galaxies and radial BAO measure [17, 18, 50]. This method is termed

as the differential approach for constraining cosmic curvature [16]. Sapona et.al (2014) test the efficiency of the method with four different statistical methods [15]. Many combinations of observational datasets have been applied on this null test but all the combinations demonstrate their consistency with the FLRW Universe and even support the flatness of Universe within different confidence regions [19–21]. Though many efforts have been made to measure Ω_k^0 using various observational datasets, there is always a need to use a model independent dataset. In earlier works comoving distances were frequently obtained by using the SNe Ia dataset. This is matter of debate since itself depends upon the dark energy model and also infected with systematic errors like cosmic opacity. However in this work we obtain the comoving distance r using the age of galaxies [12] and combine it with the selected Hubble data points(see Table2) to obtain a model independent bound on the cosmic curvature Ω_k^0 at different redshifts.

Our approach is model independent completely because the measurement of ages of old passively evolving galaxies relies only the detailed shape of the galaxy spectra but not on the galaxy luminosity [51]. Further to study the global behavior and to constrain the Ω_k^0 we apply a non parametric technique Gaussian Process and obtain a smoothened curve for it as shown in Fig.2. By analyzing this smoothened curve, we conclude that:

• From Fig. 2 it is clear that the cosmic curvature in the redshift range $0 < z < 1.37$ remains constant which in turn supports the FLRW Universe and a homogenous Universe. We can also infer that this null test disallows the possibility of an inhomogeneous Universe. However, the best fit line slightly moves away from the $\Omega_k^0 = 0$ line. However the Ω_k^0 at $z = 0$ became equal to -0.22 ± 0.58, that supports the flat universe within 1σ. The reconstructed line of Ω_k^0 also lies close to zero and completely enclose the $\Omega_k^0 = 0$ within the 1σ confidence region and thus shows consistency with the assumption of homogeneity of Universe and also in concordance with the bounds on Ω_k^0 obtained from different observations.

4.2 Method II

In this method, we use another approach to constrain the curvature of the Universe which is based on the FLRW metric. TOG (1984) [34], Gott, Park & Lee (1989) [13], Fukugita et. al. (1992) [38] and Lee et.al(1994) [42] construct the framework where statistical properties of gravitational lenses can be used to constrain the deceleration parameter and the cosmological constant.

Park & Gott [PG] (1997) [36] and Helbig [35] first proposed the use of statistical properties of gravitational lenses as a cosmological test for the curvature of Universe. PG used a dataset of 20 multiple-image lens systems [52, 53] and observed a strong negative correlation between the image separation and the source redshift. In order to search for the possible cause of this, they tried to study the effect of the evolution of lensing galaxies, clusters and curvature of the Universe on the image separation of lenses [36,54]. However, Helbig [35] showed that in an inhomogeneous universe a negative correlation is expected regardless of the value of cosmic curvature and argued that PG had used an inhomogeneous sample of gravitational lenses from the literature. Khare et. al.(2001) [43] further extended this analysis by using a dataset of 39 QSO lens systems of CfA/ Arizona Space Telescope Lens Survey [CASTLES] [55] and found no significant correlation (weak negative correlation).

In this work, we use the image separation data of lensed quasars in two different ways. First we divide the data into different redshift bins. After that we apply the GP smoothening technique to understand the variation of $\Delta\theta$ w.r.t. redshift. Second, we apply a different statistical test on the complete data of 44 points of image separation in order to explain the possible correlation between the two variables ($\Delta\theta$ and z_S) .

The brief summary of the result is as follows:

• In Fig.5, the best-fit line which represents the normalized mean image separation shows some deviation from the flat Universe . However within the 2σ region it partially incorporates the flat universe. This small inclination of best-fit towards the closed universe can't be directly taken as the deviation from

the flat Universe. Han et. al. (2014) [37] have shown that the mean image separation in the presence of direct or indirect angular selection bias or from selection bias due to the limiting magnitude on the lens shows its inclination towards positive side with increasing source redshift. Hence the deviation of the reconstructed curve in Fig.5 may be a result of several selection criterion in the formation of the dataset which can give rise to a definite bias in our result.

• Though the different bin sizes result in a difference in the number of data points, the overall trend remains the same and with a small bin-size we obtain comparatively tight bands. From this we can argue that in future with the availability of more observations, the bin-sizes can be reduced and more precise constraints can be obtained on cosmic curvature using the same method. We also believe that this test could serve as a new window to study the cosmic curvature in an model independent way.

• In order to quantify the correlation if any, we apply Pearson product-moment correlation , Spearman rank correlation test and Kendall rank correlation test on the image separation versus redshift dataset (as shown in Table 1). Contrary to the previous work [36, 43], we observe a weak positive correlation between the variables. This result is further consistent with reconstructed curve of the normalized mean image separation vs source redshift by using GP (See Fig 5).

Finally we conclude that both methods used in this work support the established flat homogeneous model of the Universe. Method I probes the assumptions of FLRW Universe and homogeneity of universe and we observe that it confirms both the assumptions. Hence in this work Method I prepares a base for Method II, as this method uses the FLRW Universe as a core assumption to obtain a measure of the curvature of the Universe. This indirect test of gravitational lenses show the consistency with flat Universe within the 2σ confidence region (see Fig.5). However the best fit line shows deviation from the flat Universe prediction which could be due to the effect of selection effects as explained above. In near future with the availability of large datasets from the surveys, we would be able to put some very tight bounds on the cosmic curvature using the same model independent and geometric tests.

Acknowledgements: Authors are thankful to Myeong- Gu Park and Phillip Helbig for useful discussions. A.R. acknowledges support under a CSIR-JRF scheme (Govt. of India, FNo. 09/045(1345/2014-EMR-I)) and also thanks IRC, University of Delhi for providing research facilities. A.M. thanks Research Council, University of Delhi, Delhi, India for providing support under R & D scheme 2015 -16.

References

[1] E. Komatsu et. al., *WMAP collaboration, Seven-Year Wilkinson Microwave Anisotropy Probe (WMAP) Observations: Cosmological Interpretation*, ApJ Suppl. 192 (2011) 18. [arXiv:1001.4538]

[2] P.A.R. Ade et al., *Planck Collaboration, Planck 2015 results. XIII. Cosmological parameters*, A&A 594 (2016) A13. [arXiv:1502.01589]

[3] C. Clarkson, B.A. Bassett & T.H. Lu, *A general test of the Copernican Principle*, PRL 101 (2008) 011301. [arXiv: 0712.3457]

[4] C. Clarkson, M. Cortes, & B. Bassett, *Dynamical Dark energy or simply cosmic curvature*, JCAP 07 (2007) 08. [arXiv:0702670]

[5] F.X. Dupe, A. Rassat, J.L. Starck & M. J. Fadili, *Measuring the Integrated Sachs Wolfe Effect*, A&A 534 (2011) A51. [arXiv:1010.2192]

[6] J.D. Barrow & F. J. Tipler, *The Anthropic Cosmological Principle* , ISBN: 978-0192821478, Oxford publication.

[7] T. Buchert & M. Carfora, *On the curvature of the present day Universe*, Class. Quant. Grav. 25 (2008) 195001. [arXiv:0803.1401]

[8] H. Skarke, *Inhomogeneity implies Accelerated Expansion*, PRD 89 (2014) 043506. [arXiv:1310.1028]

[9] M. Kleban & M. Schillo, *Spatial Curvature Falsifies Eternal Infation*, JCAP 06 (2012) 029. [arXiv:1202.5037]

[10] A.H. Guth & Y. Nomura, *What can the observation of nonzero curvature tell us?*, PRD 86 (2012) 023534. [arXiv: 1203.6876]

[11] A. H. Guth, D.I. Kaiser & Y. Nomura, *Inflationary Paradigm after Planck 2013*, PLB 733 (2014) 112. [arXiv: 1312.7619]

[12] R.F.L. Holanda, J.F. Jesus & M.A. Dantas, *Age of old objects constraints on cosmic opacity* (2016). [arXiv:1605.01342]

[13] J.R. Gott, M.G Park & H.M. Lee, *Setting limits on q0 from gravitational lensing*, ApJ 338 (1989) 12.

[14] N. Inada et.al, *The Sloan Digital Sky Survey Quasar Lens Search. V. Final Catalog from the Seventh Data Release*, ApJ 143 (2012) 119. [arXiv: 1203.1087]

[15] D. Sapone, E. Majerotto & S Nesseris, *Curvature vs Distance: testing the FLRW cosmology*, PRD 90 (2014) 023012. [arXiv: 1402.2236]

[16] E. Mortsell & J. Jonsson, *A model independent measure of the large scale curvature of the Universe.* [arXiv:1102.4485]

[17] Y.L. Li et. al., *Model-Independent Determination of Curvature Parameter Using H(z) and DA (z) Data Pairs from BAO Measurements*, ApJ 789 (2014) 15. [arXiv:1404.0773]

[18] H. Yu & F.Y. Wang, *New Model independent method to test the Curvature of the Universe*, ApJ 828 (2016) 85. [arXiv:1605.02483]

[19] R.G. Cai, Z.K. Guo & T. Yang, *Null test of the cosmic curvature using H(z) and supernovae data*, PRD 93 (2016) 043517. [arXiv:1509.06283]

[20] J.J Wei & X.F. Wu, *An Improved Method to Measure the Cosmic Curvature* (2016). [arXiv:1611.00904]

[21] Z. Li, G.J. Wang, K. Liao, Z.H. Zhu, *Model-independent estimations for the curvature from standard candles and clocks* (2016). [arXiv: 1611.00359]

[22] L.H. Benjamin & A. Shafieloo, *Model-independent test of the FLRW metric, the flatness of the Universe, and non-local measurement of* H_0. [arXiv:1606.06832]

[23] J.J. Wei at.el., *The age redshift relationship of old passive galaxies.*, ApJ 150 (2015) 35. [arXiv: 1505.07671]

[24] M.A. Dantas et. al., *Current lookback time-redshift bounds on dark energy*, PLB 679 (2009) 423. [arXiv:0901.2327]

[25] M.A. Dantas et al., *Time and distance constraints on accelerating cosmological models* , PLB 699 (2011) 239. [arXiv: 1010.0995]

[26] L. Samushia et.al, *Constraints on dark energy from the lookback time versus redshift test* , PLB 693 (2010) 509. [arXiv:0906.2734]

[27] R.G. Abraham et al., *The Gemini Deep Deep Survey. I. Introduction to the Survey, Catalogs, and Composite Spectra*, ApJ 127 (2004) 24. [arXiv: 0402436]

P.J. McCarthy et al., *Evolved Galaxies at* $z > 1.5$ *from the Gemini Deep Deep Survey: The Formation Epoch of Massive Stellar Systems*, ApJ 614 (2004) 09. [arXiv: 0408367]

[28] T. Treu et. al., *A NICMOS search for high redshift elliptical galaxy candidates*, ApJ 524 (1999) 27. [arXiv: 9907178]

T. Treu et. al., *The properties of field elliptical galaxies at intermediate redshift. I: empirical scaling laws*, MNRAS 308 (1999) 1037. [arXiv: 9904327]

T. Treu et. al., *The properties of field elliptical galaxies at intermediate redshift. 2. photometry and spectroscopy of an hst selected sample*, MNRAS 326 (2001) 221. [arXiv: 0104177].

[29] R. Jimenez et. al., *Synthetic stellar populations: Single stellar populations, stellar interior models and primordial proto-galaxies*, MNRAS 349 (2004) 240. [arXiv:0402271]

[30] J. Simon, L. Verde & J. Jimenez, *Constraints on the redshift dependence of the dark energy potential*, PRD 71 (2005) 123001. [arXiv: 0412269]

[31] A.G. Riess et. al., *A 2.4% Determination of the Local Value of the Hubble Constant*,ApJ 826 (2016) 56. [arXiv:1604.01424]

[32] M. Seikel, C. Clarkson & M. Smith, *Reconstruction of dark energy and expansion dynamics using Gaussian processes*, JCAP 06 (2012) 036. [arXiv: 1204.2832].

[33] C. E. Rasmussen & C.K.I. Williams, *Gaussian Processes for Machine Learning*, ISBN 026218253X.c MIT Press (2006), . *www.GaussianProcess.org/gpml*

[34] E.L. Turner, J.P. Ostriker & J.R. Gott, *The statistics of gravitational lenses - The distributions of image angular separations and lens redshifts*, ApJ 284 (1984) 01.

[35] P. Helbig, *The $\Delta\theta - z_s$ relation for gravitational lenses as a cosmological test*, MNRAS 298 (1998) 02. [arXiv:9804104]

[36] M.G. Park & J.R Gott, *Curvature of the Universe and observed gravitational lens image separation vs. redsgift*, ApJ 489 (1997) 476. [arXiv: 09702173]

[37] D.H. Han & M.G. Park, *Constraining cosmology with image separation statistics for gravitationally-lensed quasars in the Sloan Digital Sky Survey*, Jour. Korean Astron. Soc. 65 (2014) 827.

[38] M. Fukugita, T.Futamase, M Kasai & E.L. Turner, *Statistical properties of gravitational lenses with a nonzero cosmological constant*, ApJ 393 (1992) 03.

[39] A.Dev, D.Jain & S.Mahajan, *Dark Energy and the statistical study of the observed image separations of the multiply imaged systems in the class statistical sample*, IJMPD 13 (2004) 06. [arXiv:0307441]

[40] R. Kayser, P. Helbig & T. Schramm, *A General and practical method for calculating cosmological distances*, ApJ 318 (1997) 680. [arXiv: 9603028]

[41] C. Keeton, *A Catalog of Mass Models for Gravitational Lensing*, ArXiv Astrophysics e-prints. [arXiv:0102341]

[42] H.A. Lee, & M.G. Park, *Statistical properties of gravitational lanes in cosmological models with cosmological constant*, Jour. Korean Astron. Soc. 27 (1994) 103.

[43] P. Khare, *Angular separations of lensed quasar images*, ApJ 550 (2001) 153.

[44] W.H. Press, S.A. Teukolsky, W.T. Vetterling & Brian P. Flannery; Numerical Recipes in C [ISBN-13: 978-0521431088], Cambridge University Press.

[45] G. Bernstein, *Metric Tests for Curvature from Weak Lensing and Baryon Acoustic Oscillations*, ApJ 637 (2006) 598. [arXiv: 0503276]

[46] S. Rasanen, K. Bolejko & A. Finoguenov, *New Test of the Friedmann-Lematre-Robertson-Walker Metric Using the Distance Sum Rule*, PRD 115 (2015) 101301. [arXiv:1412.4976]

[47] T. Buchert; A.A. Coley, H. Kleinert, B.F. Roukema,D.L. Wiltshire, *Observational challenges for the standard FLRW model*, IJMPD 25 (2016) 244 [arXiv:1512.03313]

[48] D. L. Wiltshire, *Average observational quantities in the timescape cosmology*, PRD 80 (2009) 123512. [arXiv:0909.0749]

[49] C. Boehm & S. Rasanen, *Violation of the FRW consistency condition as a signature of backreaction*, JCAP 09 (2013) 003. [arXiv:1305.7139]

[50] A. Shafieloo & C.Clarkson, *Model independent tests of the standard cosmological model*, PRD 81 (2010) 083537. [arXiv:0911.4858]

[51] A. Avgoustidis, L. Verde & R. Jimenez, *Consistency among distance measurements: transparency, BAO scale and accelerated expansion*, JCAP 09 (2009) 06. [arXiv:0902.2006]

[52] J. Surdej & G. Soucail, *in Gravitational Lenses in the Universe, ed. by J. Surdej, D.Fraipont-Caro, E. Gosset, S. Refsdal, & M. Remy*, Li ege, Universitede Liege 205 (1994).

[53] C.R. Keeton & C.S. Kochanek, *in Astrophysical Applications of Gravitational Lensing*, I.A.U. Symp. no. 173 (1996).

[54] S.Y. Yoon& M.G. Park, *Statistics of Gravitational Lensing by a Galaxy in Cluster or in Field*, Jour. Korean Astron. Soc. 29 (1996) 119.

[55] CASTLES; CfA/ Arizona space telescope lens survey; *https://www.cfa.harvard.edu/castles/*

[56] C. Zhang et al., *Four New Observational H(z) Data From Luminous Red Galaxies of Sloan Digital Sky Survey Data Release Seven*, RAA. 14 (2014) A10. [arXiv: 1207.4541]

[57] R. Jimenez, L.Verde, T. Treu & D. Stern, *Constraints on the equation of state of dark energy and the Hubble constant from stellar ages and the CMB*, ApJ 593 (2003) 622. [arXiv: 0302560]

[58] M. Moresco et al., *Improved constraints on the expansion rate of the Universe up to* $z \sim 1.1$ *from the spectroscopic evolution of cosmic chronometers*, JCAP 08 (2012) 006 [arXiv: 1201.3609]

[59] E. Gaztanaga, A. Cabre & L. Hui, *Clustering of Luminous Red Galaxies IV: Baryon Acoustic Peak in the Line-of-Sight Direction and a Direct Measurement of H(z)*, MNRAS 399 (2009) 1663. [astro-ph/0807.3551]

[60] X. Xu et al., *Measuring* D_A *and H at z=0.35 from the SDSS DR7 LRGs using baryon acoustic oscillations*, MNRAS 431 (2013) 2834. [arXiv: 1206.6732]

[61] M. Moresco et al., *A 6% measurement of the Hubble parameter at* $z \sim 0.45$*: direct evidence of the epoch of cosmic re-acceleration*, JCAP 05 (2016) 14. [arXiv: 1601.01701]

[62] C. Blake et.al., *The WiggleZ Dark Energy Survey: the growth rate of cosmic structure since redshift z=0.9*, MNRAS 425 (2012) 405. [arXiv:1104.2948]

[63] D. Stern et al., *Cosmic Chronometers: Constraining the Equation of State of Dark Energy. I: H(z) Measurements*, JCAP 02 (2010) 08. [arXiv: 0907.3149]

[64] L. Samushia et al., *The Clustering of Galaxies in the SDSS-III DR9 Baryon Oscillation Spectroscopic Survey: Testing Deviations from* Λ *and General Relativity using anisotropic clustering of galaxies*, MNRAS 429 (2013) 1514. [arXiv: 1206.5309]

[65] M. Moresco, *Raising the bar: new constraints on the Hubble parameter with cosmic chronometers at* $z \sim 2$, MNRAS 450 (2015) 16. [arXiv:1503.01116]

Sr.no	z	H(z)	σ_H	Reference	Method and data used	Comment
1	0.070	69	19.6	[56]	SDSS DR7	R
2	0.090	69	12	[57]	GDDS+RG	R
3	0.120	68.6	26.2	[56]	SDSS DR7	A
4	0.170	83	8	[30]	GDDS+RG+SPEED	R
5	0.179	75	4	[58]	D4000 GSA	A
6	0.199	75	5	[58]	D4000 GSA	A
7	0.200	72.9	29.6	[56]	SDSS DR7	A
8	0.240	79.69	2.65	[60]	BAO	A
9	0.270	77	14	[30]	GDDS+RG+SPEED	R
10	0.280	88.8	36.6	[56]	SDSS DR7	A
11	0.350	84.4	7	[60]	BAO	A
12	0.352	83	14	[58]	D4000 GSA	A
13	0.380	83	14	[61]	BOSS DR-9	A
14	0.400	95	17	[30]	GDDS+RG+SPEED	R
15	0.4004	77	10.2	[61]	BOSS DR-9	A
16	0.4247	87.1	11.2	[61]	BOSS DR-9	A
17	0.43	86.45	3.68	[59]	BAO	A
18	0.44	82.6	7.8	[62]	BAO	A
19	0.445	92.8	12.9	[61]	BOSS DR-9	A
20	0.4783	80.9	9	[61]	BOSS DR-9	A
21	0.480	97	62	[63]	SDSS LRDs + KC	A
22	0.57	92.4	4.5	[64]	BAO	A
23	0.593	104	13	[58]	D4000 GSA	A
24	0.60	87.9	6.1	[62]	BAO	A
25	0.680	92	8	[58]	D4000 GSA	A
26	0.73	97.3	7.0	[62]	BAO	A
27	0.781	105	12	[58]	D4000 GSA	A
28	0.875	125	17	[58]	D4000 GSA	A
29	0.880	90	40	[63]	SDSS LRDs + KC	A
30	0.900	117	23	[65]	GDDS+RG+SPEED	R
31	1.037	154	20	[58]	D4000 GSA	A
32	1.300	168	17	[65]	GDDS+RG+SPEED	R
33	1.363	160	33.6	[65]	D4000 GSA	A
34	1.430	177	18	[65]	GDDS+RG+SPEED	R
35	1.530	140	14	[65]	GDDS+RG+SPEED	R
36	1.750	202	40	[65]	GDDS+RG+SPEED	R

Table 2: 36 Hubble data points measured using passively evolving galaxies. R- removed, A - allowed